

INVESTIGATION OF LIQUID PHASE CHARACTERISTICS IN A FALLING FILM MICROREACTOR

A.D. Anastasiou¹, A. Gavriilidis², A.A. Mouza^{1*}

¹Department of Chemical Engineering, Aristotle University of Thessaloniki, Greece

²Department of Chemical Engineering, University College London, UK

* tel.: +30 2310 994161; Fax: +30 2310 996209; Email: mouza@auth.gr

ABSTRACT

One of the most important variables in the designing of gas-liquid reactors is the required interfacial area between gas and liquid phases. Falling film microreactors (*FFMR*) are devices which can offer extended specific surfaces (up to 20,000 m²/m³) and for this reason they are used for many multiphase processes. In the present work the geometrical characteristics of the liquid phase in a *FFMR* are studied using a micro Particle Image Velocimetry system (μ -*PIV*). The experiments were conducted in microchannels with widths of 1200, 600 and 300 μ m and for *Reynolds* numbers between 0.9 and 31.5. In order to validate this method a comparison between the experimental data and an expression for predicting the meniscus shape in a capillary tube was made. As gravity effects are minimized in the microscale and surface tension tends to play a more significant role, well known equations of macroscale are expected to be invalid in microscale. With the aim of confirming this assumption the findings for liquid phase thickness were compared with values predicted using the expressions of Nusselt and Kapitza.

INTRODUCTION

During the last decade many researchers have worked on system miniaturization and process intensification, aiming to build more compact, smaller, cheaper and more efficient equipment. As a result many works dealing with the operation parameters of microfluidic systems have been published. In general, microfluidics refers to the study and manipulation of liquid and gas flows in channels and geometries which have at least one characteristic dimension that is less than one millimeter and above one micrometer. There are several differences in physical behavior observed between the macro and micro worlds of fluid mechanics. These differences are best explained by considering the different forces which govern the flow in each case. Due to the small characteristic dimension of the conduit, the typical *Reynolds* numbers (*Re*) in microsystems are low, viscous forces dominate the flow, while inertial forces become less important. At the same time the ratio of surface area to system volume increases and so does the relative importance of surface forces. Additionally, as the interfacial area is greater, heat and mass transfer rates are enhanced. Nowadays, microfluidics covers a large variety of applications, e.g., detection and control of chemical reactions, sample preparation, flow and pressure sensors, microequipment for mixing, separation or heating, microscale systems for biological diagnostics as DNA analysis, pumping systems [1]. Microsystems are characterized by low consumption of reagents, quick system response as well as multifunctionality since many unit operations can be combined in a single piece of equipment. Alternative energy fields, such as

electromagnetic, acoustic, electric, gravitational or capillary forces could be also applied to generate fluid flow [1]. One main challenge in the application of microequipments is their use for large scale production. The simplest way to achieve this is by numbering-up relevant flow features such as the number of the channels, or by smart increasing of dimensions like the length of the channels.

Of great interest in microfluidics is the study of multiphase systems in microchannels. The liquid and gas phase can be either dispersed or separated. Although in both cases high specific areas can be obtained, in falling film microreactors (*FFMR*) stable and well controlled interface is also assured [2]. In microchannels the film is quite stable and might have a thickness of less than 100 μm while in conventional falling film systems the film thickness is about 0.5 to 3mm. As such thin films offer high heat and mass transfer capabilities *FFMR* are suitable for many applications (e.g. reaction, extraction, evaporation and highly exothermic processes). The majority of the published work concerning *FFMR* deals with the conversion rate of specific reactions, e.g. [3-5], while little work has been published concerning the characteristics of the interface. Al-Rawashdeh[6] et al., have numerically investigated the effect of liquid flow distribution, gas chamber height and hydrophilic-hydrophobic channel material. To the authors' best knowledge only Yeong et al. [7] have investigated experimentally the shape of the interface and the liquid film thickness using laser scanning confocal microscopy.

As the design and production time for complex microreactors is considerably long [8], it is important to be able to understand and predict the flow phenomena as well as the parameters which affect their operation in order to be able to ensure easy fabrication and optimal operation. However, none of the aforementioned works propose either a design strategy for *FFMR* or an expression for predicting the liquid phase characteristics in the system. This work is part of a project concerning the study of flow characteristics in micro-channels. The aim of the present work is to study the geometrical characteristics of the falling film and to investigate the parameters that affect them, using a novel measuring technique.

Methods for film thickness measurement

The development of reliable non-intrusive methods for liquid film measurements is very important in the area of multiphase flow. Several non-intrusive methods have been proposed for conducting liquid film measurements in two phase systems. Tibirićá et al. [9] in their review work classified them as follows:

- acoustic, which are based on ultrasound waves
- electrical, where electrodes measure the conductivity in liquid phase
- optical, which are based on the detection of the interface as the light emitted by each phase present different characteristics
- absorption by the fluid or different types of radiation

Although all the aforementioned methods are suitable for macrosacale applications, they might not be applicable in the microscale for various reasons. For example, special probes (like electrodes) may not possible to be mounted to the channel walls, while the small liquid volume might render the generated signals too weak to be successfully detected and measured. In this work micro Particle Image Velocimetry ($\mu\text{-PIV}$), a common optical non-intrusive method for measuring two-dimensional velocity fields, is going to be also applied for estimating the thickness of the liquid phase and defining the shape of the interface.

It is known that $\mu\text{-PIV}$ is an effective technique for obtaining instantaneous two-dimensional velocity measurements in microchannels with high spatial resolution and accuracy. To conduct the measurements the fluid must be initially seeded with tracer particles that are generally assumed to follow the flow. Consequently, the seeding particles must be small enough to follow the fluid motion accurately and to avoid microchannel obstruction and at the

same time large enough to be successfully imaged and to avoid Brownian motion. Fluorescent techniques can also be applied for ensuring better particle visibility and for removing the background noise. Two successive particle images must be acquired over a known time interval, Δt , for each measurement (**fig. 1a**). Each of these images is divided into smaller regions called *interrogation areas*. To facilitate the analysis, the initial image must be further processed. After correcting the light sheet non-uniformities (**fig. 1b**), the noise is reduced by subtracting the background image. As a result only the tracing particles remain visible (**fig. 1c**).

The displacement of a group of particles is determined by employing in every interrogation region a cross-correlation technique. The local velocity is finally calculated from the estimated displacement (ΔS) over a time interval (Δt). Combining the data from each interrogation region a two-dimensional vector map of the flow is obtained (**fig. 1d**).

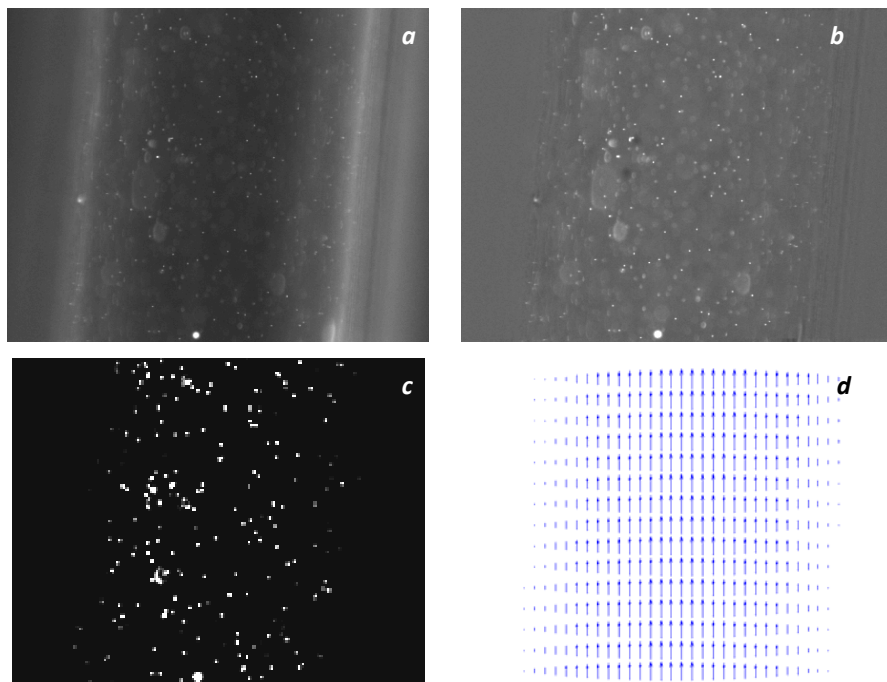


Figure 1: The process of a μ -PIV measurement; a) one of the two initial images of the flow; b) The effect of image balancing; c) Signal amplification; d) Two-dimensional vector map.

As the dimensions of the systems investigated are in microscale, the flow should be imaged with sufficiently high magnification and with high diffraction resolution optics. For this reason a microscope with appropriate objective lens is used. The most common microscope objective lenses range from diffraction-limited oil-immersion lens with magnification (M) equal to 60, and numerical aperture (NA) equal to 1.4, to low magnification air-immersion lens with $M=10$ and $NA=0.1$. From these technical characteristics important parameters such as the *spatial resolution* and the *depth of field* or more appropriately the *depth of the correlation* are defined. Spatial resolution describes how clearly the particles are imaged. For high numerical aperture and high magnification the particles are resolved with at least three or four pixels across their diameter. While the depth of field refers to the distance a point source of light may be away from the focal plane and still produce an acceptably focused image, the depth of correlation refers to

how far from the focal plane a particle will contribute significantly to the correlation function (*fig. 2*). The narrower the depth of correlation the more velocity measurements can be taken resulting to more detailed velocity profiles. This can be achieved by varying the height in which microscope is focused and by taking measurements on more planes. As the flow is laminar and the concept of continuity is valid a reconstruction of a 3D vector field can be made by combining the data obtained from each plane, as also suggested by Meinhart [10].

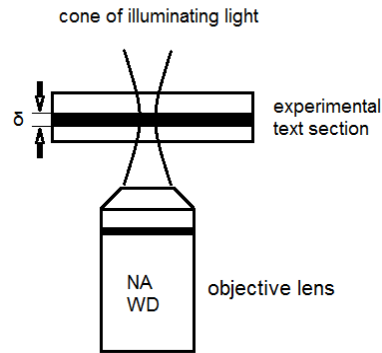


Figure 2: Depth of field (δ) of an objective lens.

EXPERIMENTAL SETUP

All experiments were conducted in three square-cross-section microchannels ($D_1=1200 \mu\text{m}$, $D_2=600 \mu\text{m}$, $D_3=300 \mu\text{m}$) and a length of 1200 mm (*fig. 3*). The test section is micromachined on polymeric material. The liquid phase first overflows a circular region constructed at the inlet of each microchannel, so as the continuous free flow of the liquid phase to be assured.

A fluorescent μ -PIV system was used to study the flow (*fig. 4*). The measuring section of the microchannel was illuminated by a double cavity laser emitting at 532 nm. The flow was recorded using a high sensitivity CCD camera, connected to a Nikon microscope. The light source was synchronized with the camera shutter by a timer box. The flow was traced by adding fluorescent polystyrene particles with mean diameter of $1 \mu\text{m}$. In order to obtain magnified images a 20X air immersion objective with $NA=0.20$ was used and this corresponds to $8 \mu\text{m}$ depth of correlation. The time delay between frames lies in the range of 150-1500 μs , depending on the flow rate studied each time, while the sampling rate was 5 Hz. For every measurement 100 images were acquired and the vector maps were estimated by averaging these images. Finally, the image processing and the velocity estimations were performed using the *Flow Manager Software (DantecDynamics)*.

Distilled water was used as working fluid which was circulated by means of a syringe pump. The surface tension of water, measured using a tensionmeter (*Cam200 optical contact angle meter*), was found to be 72 mN/m, while the contact angle between the liquid and the polymeric material of the microchannels is measure to be 62 deg. The test section was placed in an inclined position of 25 deg from the horizontal. To eliminate entrance phenomena the measurements were conducted 40 mm downstream from the inlet of the microchannels.

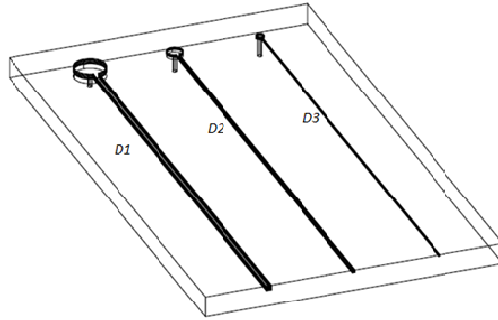


Figure 3: Geometry of the microchannels used for the experiments ($D_1=1200\mu\text{m}$, $D_2=600\mu\text{m}$, $D_3=300\mu\text{m}$).

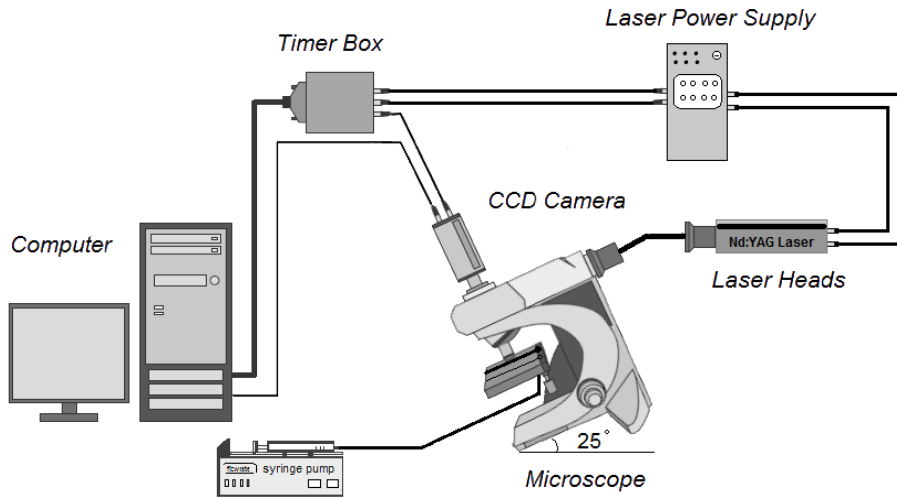


Figure 4: Experimental setup used for measuring film thickness.

RESULTS AND DISCUSSION

The geometrical characteristics of the liquid phase were investigated by employing the μ -PIV system and taking advantage of the narrow depth of field, which permits focusing and taking measurements on different planes. Since during the measurements the liquid phase is seeded with light emitting particles, the interface between liquid and gas phase can be easily distinguished on an image of the flow conduit (**fig. 5a**). The dark region between the two groups of particles is the gas phase, while the outer dark regions correspond to the walls of the microchannel. The distance between the wall and the gas phase is the width of the liquid phase (W). The top of the interface coincides with the plane where the first particles can be observed (plane A at **fig. 5b**). At this point, the liquid phase covers a very narrow region (**fig. 6a**). As the focusing plane is moving closer to the bottom wall (e.g. **fig. 5**, intermediate plane), with a step

of 10 μm , this region broadens (*figs. 6b, 6c, and 6d*) until the point where the two liquid regions are close to merge (*fig. 6e*). The first plane where only the liquid phase can be observed (*fig. 6f*) is recognized as the ending point of the gas-liquid interface. The shape of the interface can be reconstructed by combining the liquid phase width (W) measurements on consecutive planes (*fig. 7a*). As expected a meniscus is formed due the hydrophilicity of the microchannel material (contact angle 62 deg) and the fact that in such small conduits capillary forces play an important role.

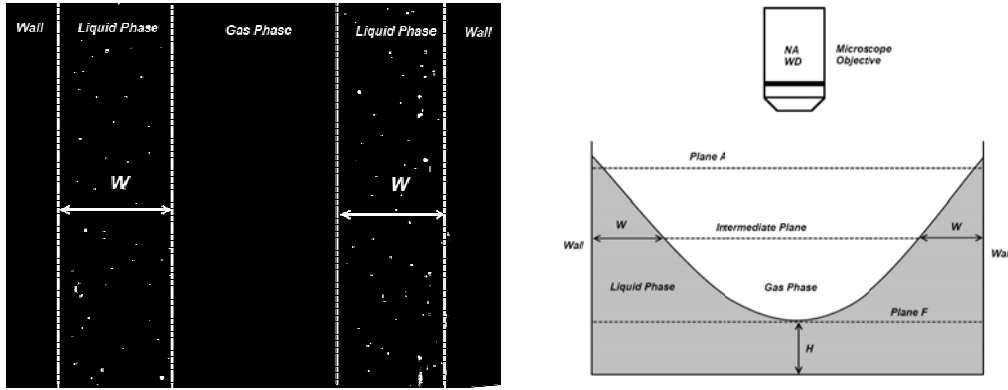


Figure 5: Typical μ -PIV image. Schematic defining the walls, the liquid and the gas phase.

In *fig. 7b* a photo of the liquid phase is presented. It must be noted that due to the small conduit dimensions and the lighting conditions the photo is not clear. However, it is indicative of the shape of the interface, which is clearly similar to that predicted using the μ -PIV measurements. An expression which defines the shape of the meniscus formed in capillary tubes (*Eq. 1*) [11] seems to fit the data satisfactorily (*fig. 8*), although it is not intended for flowing liquid phase. This expression takes into account the properties of the liquid phase (surface tension and density) as well as the effect of the gravitational forces.

$$h(w) = -\sqrt{\frac{\sigma}{\rho g}} \operatorname{argch} 2 \sqrt{\frac{\sigma}{\rho g w^2}} + \sqrt{\frac{2\sigma}{\rho g}} \sqrt{2 - \frac{\rho g w^2}{2\sigma}} + \text{const} \quad (1)$$

Apart from the shape of the interface, the thickness (H) of the liquid phase (*fig. 5b*) has been also measured. Starting from the last plane of the interface (*plane D, fig. 5b*) the focusing plane is moved towards the bottom wall of the channel with a step of 20 μm , until no particles can be observed. This is regarded as the bottom of the microchannel and the distance measured is the minimum thickness (H) of the liquid phase. Measurements are conducted for the three microchannels and for *Reynolds* numbers in the range of 0.9 to 31.5. In *figs 9a* and *9b* the experimental data obtained for channel widths 1200 μm and 600 μm respectively, are compared with values predicted by the correlations proposed by Nusselt (*Eq.2*) and Kapitza (*Eq. 3*). It must be however pointed out that these expressions do not take into account the effect of the side walls and the surface phenomena on the liquid film.

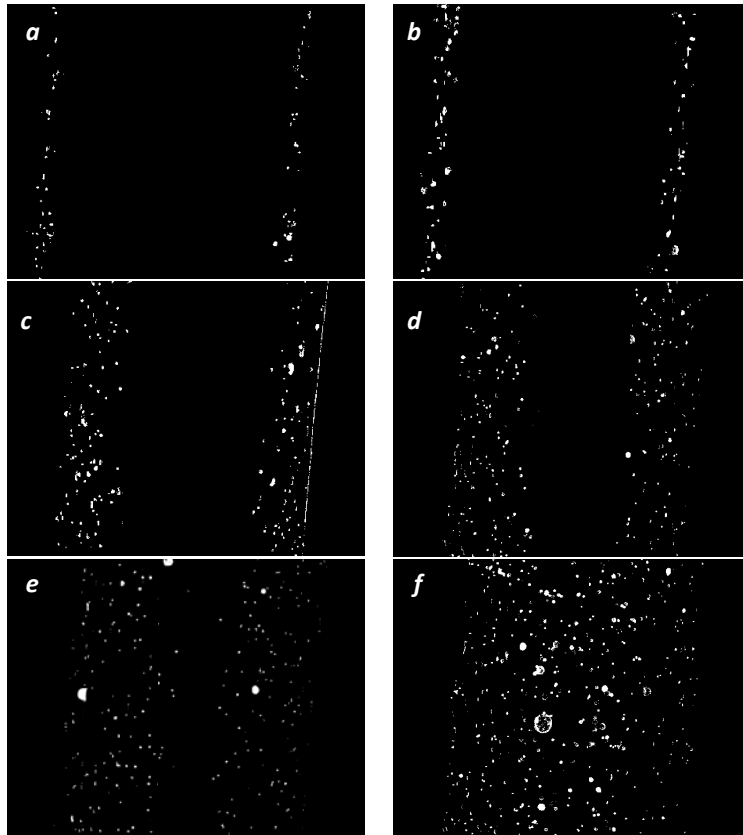


Figure 6: Images of gas-liquid interface at the microchannel of 600 μm .
 a) Plane A, b), c), d), e) Intermediate planes, f) Plane F.

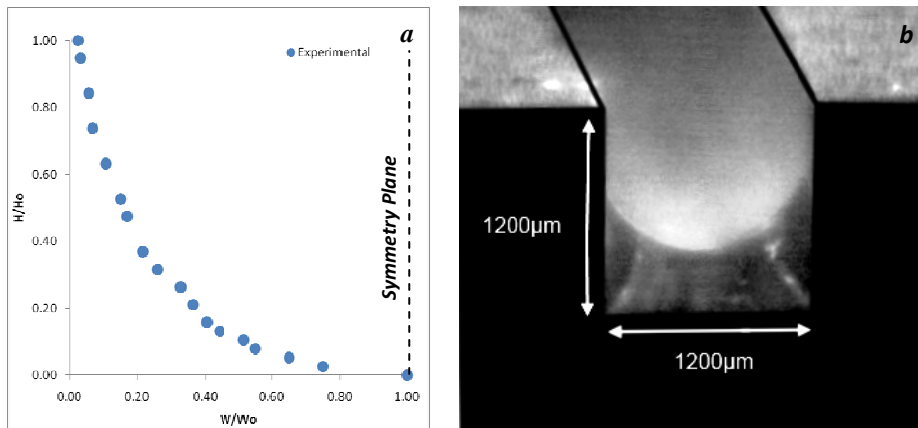


Figure 7: Shape of the gas-liquid interface: a) Experimental results ($D=1200 \mu\text{m}$, $Re=13.5$);
 b) Typical photograph of the meniscus.

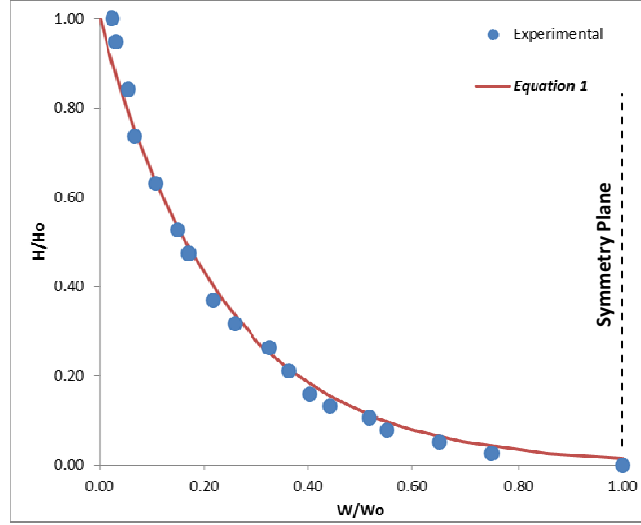


Figure 8: Meniscus shape. Comparison between experimental data and theoretical expression ($D=1200 \mu\text{m}$, $Re=7.2$).

It can be observed that for the larger microchannel (*fig. 9a*) the values predicted by *Eq. 2* are higher than the experimental ones. It is obvious that the higher difference exist for the lower flow rates employed (*fig. 9a*) while as Re becomes higher the difference becomes smaller. On the other hand for D_2 and low Re the deviation between experiments and theory is very small (*fig. 9b*). At high Re the values predicted by correlations are lower than experimental ones, while the difference can be even higher than 100% (141% for $Re=20.4$). In the case of the smaller microchannel even at low Re the thickness measured is about 50% higher than the predicted one (*table 1*). In *fig. 10*, the measured film thickness for $D_1=1200 \mu\text{m}$ is compared with that for $D_2=600 \mu\text{m}$. It is obvious that for the same Re the film thickness has higher values in the case of D_2 .

$$H_{Nusselt} = \left(\frac{3v^2 Re}{g \sin \theta} \right)^{1/3} \quad (2)$$

$$H_{Kapitza} = \left(\frac{2.4v^2 Re}{g \sin \theta} \right)^{1/3} \quad (3)$$

These findings can be explained by considering the relevant magnitude of the forces acting on the liquid phase. At the larger microchannel the effect of the walls is less intense and the difference between experimental results and correlations can be attributed to the existence of the meniscus. As the flow increases the film thickness (H) at the bottom also increases while the maximum height of the meniscus remains unchanged, rendering the presence of the meniscus less important. On the other hand as the width of the microchannels become smaller the drag forces exerted by the walls and the surface phenomena become more significant. This hinders the flow of the liquid phase and consequently increases its volume and its thickness. It is obvious that under these circumstances correlations valid in macroscale underestimate the thickness of the liquid film by 20-141%.

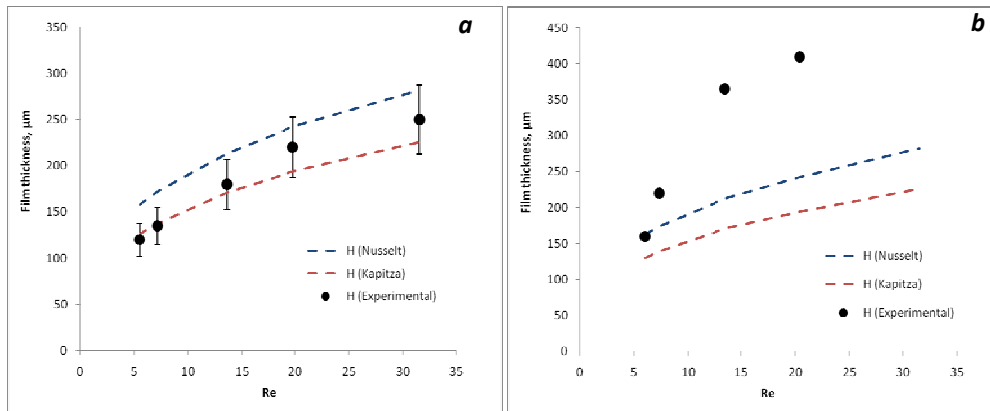


Figure 9: Comparison between experimental liquid film thickness and those predicted by correlations: a) $D_1=1200\mu\text{m}$; b) $D_2=600\mu\text{m}$.

Table 1: Comparison of film thickness (H) in three different microchannels.

Re	D (μm)	H_{exp} (μm)	$H_{Nusselt}$ (μm)	$H_{Kapitza}$ (μm)
13.5	1200	160	214	171
19.8	1200	205	242	194
13.5	600	345	213	171
20.7	600	400	246	197
0.9	300	130	85	69

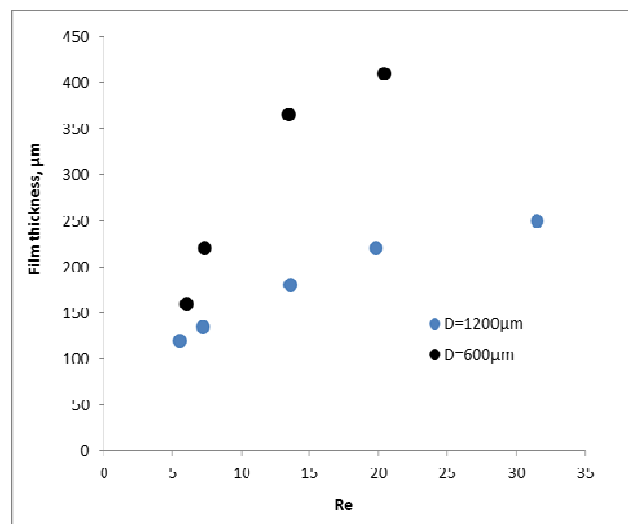


Figure 10: Comparison of the measured minimum film thickness for D_1 and D_2 .

CONCLUSIONS

The scope of this work was the study of the characteristics of the liquid phase in a *FFMR* micro-machined on hydrophilic substrate. Experiments were conducted in three microchannels ($D_1=1200\mu\text{m}$, $D_2=600\mu\text{m}$, $D_3=300\mu\text{m}$) and for Re in the range of 0.9 to 31.5. The shape of the interface, which was reconstructed by acquiring measurements on different planes using a μ -*PIV* system, confirms the existence of a meniscus, which can be attributed to the capillary forces which turn to be important in such narrow conduits. The existence of a meniscus increases the extent of the interfacial area available for gas-liquid reaction in falling film micro-reactors, which is an important parameter in the designing of *FFMR*.

Measurements of the film thickness proved that the expressions valid in macroscale are unable to predict the characteristics of the liquid phase in microchannels. In conclusion, more work is needed and is currently in progress to investigate the relative effect of all the parameters that affect the operation of a *FFMR* and to develop expressions valid in the microscale.

Acknowledgements: The authors wish to acknowledge Prof S.V. Paras (AUn), Dr H. Makatsioris (Brunel University, UK) and the Lab technician Mr. A. Lekkas for their contribution.

REFERENCES

- [1] Nguyen, N.-T. & Wereley, S.T. 2002. *Fundamentals and Applications of Microfluidics: Second Edition*, Boston, Artech House.
- [2] Ziegenbalg, D., Löb, P., Al-Rawashdeh, M.M., Kralisch, D., Hessel, V. & Schönfeld, F. 2010. Use of 'smart interfaces' to improve the liquid-sided mass transport in a falling film microreactor. *Chemical Engineering Science*, **65**, 3557-3566.
- [3] Chambers, R.D., Holling, D., Spink, R.C.H. & Sandford, G. 2001. Gas - liquid thin film microreactors for selective direct fluorination. *Lab on a Chip*, **1**, 132-137.
- [4] Chasanis, P., Lautenschleger, A. & Kenig, E.Y. 2009. CFD-based investigation of carbon dioxide absorption in a falling-film micro-absorber. *Chemical Engineering Transaction*, **18**, 593-598.
- [5] Stavarek, P., Le Doan, T.V., Loeb, P. & De Bellefon, C. 2009. Flow visualization and mass transfer characterization of falling film reactor. Proc. 8th World Congress of Chemical Engineering, Montreal, Canada.
- [6] Al-Rawashdeh, M.M., Hessel, V., Lob, P., Mevissen, K. & Schonfeld, F. 2008. Pseudo 3-D simulation of a falling film microreactor based on realistic channel and film profiles. *Chemical Engineering Science*, **63**, 5149-5159.
- [7] Yeong, K.K., Gavriilidis, A., Zapf, R., Kost, H.J., Hessel, V. & Boyde, A. 2006. Characterisation of liquid film in a microstructured falling film reactor using laser scanning confocal microscopy. *Experimental Thermal and Fluid Science*, **30**, 463-472.
- [8] Klank, H., Goranovic, G., Kutter, J.P., Gjelstrup, H., Michelsen, J. & Westergaard, C.H. 2002. PIV measurements in a microfluidic 3D-sheathing structure with three-dimensional flow behaviour. *Journal Of Micromechanics And Microengineering*, **12**, 862-869.
- [9] Tibiriçá, C.B., Do Nascimento, F.J. & Ribatski, G. 2010. Film thickness measurement techniques applied to micro-scale two-phase flow systems. *Experimental Thermal and Fluid Science*, **34**, 463-473.
- [10] Meinhart, C.D. 2007. A 3D-3C Micro-PIV Method. *Conference on Nano/Micro Engineered and Molecular Systems*. Bangkok.
- [11] Levich, V.G. 1962. *Physicochemical Hydrodynamics*, Prentice-Hall, Inc.